

## Schizocommunin analogues and derivatives as G-quadruplex ligands and anticancer agents

S. M. Bakalova, J. Kaneti\*

*Institute of Organic Chemistry with Centre of Phytochemistry, Bulgarian Academy of Sciences,  
Acad. G. Bonchev Str., Block 9, 1113 Sofia, Bulgaria*

Received: November 3, 2023; Revised: April 09, 2024

G-quadruplexes (GQs) have become valid targets for anticancer efforts in the recent couple of decades due to their extremely multifaceted biological functions. Our goal is to quantify interactions within GQs, as well as their interactions with potential ligands (Ls). As secondary nucleic acid (NA) structures, GQs may be understood as a central channel of stacked G-quartets, interlinked into a G-stem (GS) with nucleotide loops. Computational data on full GQ energetics are, however, increasingly noisy. Therefore, we have chosen to simplify our GQ model by stripping it off all nucleotide residues into a “naked” GQ. The GQ-L stacking model allows computing of intrinsic interaction energies, as well as external ligand stacking affinities with “chemical precision”. To relate computed ligand – G4 affinities to their biological activity, we use published inhibitory activities (IC<sub>50</sub> values) of several groups of heterocycles. Some of our results provide a good linear relationship between ligand stacking affinities to GQ, calculated by quantum chemical DFT methods, and corresponding log(IC<sub>50</sub>) values. Herewith we discuss the obtained results in terms of a mechanism of anticancer activity of heterocyclic ligands *via* complexation with GQs and thereby control of GQ cell regulatory activity.

**Keywords:** G-quadruplexes, nitrogen heterocyclic ligands, stacking interactions, IC<sub>50</sub> vs. G4-affinity relationship

### INTRODUCTION

Alkaloids and their chemical analogues have long been among the most popular and sought for organic natural, laboratory and industrial products for a leading reason – their beneficial physiological activity on human health [1]. Recently, their activity and use has increasingly been related to their capability to interact with a special category of nucleic acids (NAs) – the four stranded G-quadruplexes [1]. While not being directly involved in the preservation and transfer of genetic information, G-quadruplexes have been disclosed as decisive participants in a plethora of cellular processes as NA biosynthesis, replication, transcription, oncogenesis, etc. Telomeres are a known site accumulating G-quadruplexes, which are thereby essential to telomere functioning in cancer, aging and genetic stability. A G-quadruplex may inhibit telomerase activity, which directly affects cancer cells and primary tumors [2]. A G-quadruplex may dissociate telomere-binding proteins thus leading to dysfunction and finally to apoptosis or senescence [3]. A G-quadruplex interferes with telomeric replication by impairing replication fork progression [4]. Knowledge of ligand structures stabilizing G-quadruplexes allows for the specific design of heterocyclic structures targeting the cancer cell function [1, 5].

The recent decade has seen quite a number of efforts to quantify anticancer activities of series of

selected heterocycles on cultivated cancer cell cultures [1, 6, 7]. The results of these efforts outline important structure – activity trends in series of quinazoline derivatives [6], indenoisoquinoline derivatives, including an isolated MYC-cancer promoter [7], and more generally in G-quadruplexes of various functions, structures and sizes, as well as various quadruplex targeting heterocyclic ligands [8]. On the other hand, the belief that G4-ligands lack selectivity due to targeting multiple quadruplexes and thus many different sites in the genome still has a significant place in the literature [9]. This requires additional efforts to reduce effects of different binding of G4-ligands [9 and references therein], which remain very attractive therapeutic agents nevertheless [10]. Moreover, one might consider a G-quadruplex itself as determining selectivity and attracting (larger size) heterocycles to stack to its large G4 plane. In these terms, G-quadruplex selectivity with respect to crescent-shaped planar ligand chromophores has repeatedly been noticed [1, 8] and exploited in the search of novel anticancer heterocycles [11], even though the terms G-quadruplex and mechanism of action have not been mentioned together in the latter review [11]. The pressing demand to all anticancer activity studies is then the generalization of their biochemical pharmacology data in the form of IC<sub>50</sub>, that is, their structure – activity information, into quantitative form. Half-maximal inhibitory concentration (IC<sub>50</sub>) is the most widely used and

\* To whom all correspondence should be sent:  
E-mail: [jose.kaneti@orgchem.bas.bg](mailto:jose.kaneti@orgchem.bas.bg)

informative measure of a drug's efficacy. It indicates how much drug is needed to inhibit a biological process by half, thus providing a measure of potency of an antagonist drug in pharmacological research. The value of  $IC_{50}$  of a ligand regarded as its inhibition constant [12] should exponentially depend on ligands' G4 affinity. The latter value is conveniently computable theoretically.

We have ventured into the field while discussing the mechanism of biological activity of some quinazoline-4-one derivatives [13]. The latter has introduced us to the possible involvement of G-quadruplexes in the problem, and the necessity to bring up adequate computational methodologies to its solution. Traditional molecular mechanics MM and molecular dynamics MD approaches do not seem capable of bringing sufficiently accurate results for G-quadruplex structures [14]. This problem is related to both intrinsic lack of accuracy, and technical numerical noise accumulating with slow energy convergence for polyatomic structures as G-quadruplexes [14, 15]. The necessary theoretical and computational accuracy only looks achievable using large-scale quantum chemical calculations [15]. To reduce the computational problem to affordable limits and improve accuracy as much as possible, we strip our G-quadruplex model off all nucleotide residues [13]. This leaves the model a core of stacked guanine tetrads with a central channel containing the pertinent stabilizing  $K^+$  or  $Na^+$  ions [8]. With a size of 130 to 260 and more atoms, of which 64 for a single G4 quartet (C, H, N, O) atoms plus a  $K^+$  per layer, the core-G4 system is relatively easily amenable to quantum chemical calculations using density functional theory, DFT [16]. Improved "chemical precision" molecular orbital post-Hartree-Fock calculations, are feasible as well [17].

#### SELECTION OF HETEROCYCLIC COMPOUNDS AS POTENTIAL GQ-LIGANDS

Our initial work has been oriented to computational design and directed synthesis of N---H---N heterocycles, with emphasis on their capability to undergo intramolecular proton transfer, possibly related to biological activity. In this respect, quinazolines and derivatives have been considered promising. 4-Amino-quinazolines [6, 18] and perimidines [19] (entries 5, 7, 8; Table 1) have been selected as potentially convenient synthetic targets, based on extensive literature data. The interest to derivatives of schizocommunin [1], however, also stems directly from their biological mechanisms,

related to G-quadruplexes. Further structural speculations, related to GQ-drug design, led us to benzimidazolo[1.2-a] quinolines [20, 21], which are also given some attention here.

#### COMPUTATIONAL MODELING

To obtain the required DFT affinities of heterocyclic ligands to a model G-quadruplex, we mostly use the wB97XD functional, chosen for its reasonable treatment of long-range and dispersion interactions [22, 23] at the 6-31G(d,p) basis set level, as implemented in the Gaussian program system [24]. This corresponds to the expected stacking type of interactions in the layered secondary NA structures. We also test the general purpose M06-2X functional, where the hydrogen bonding and long-range interactions are well covered, but dispersion is not explicitly accounted for. We follow the routine protocol for location of minima on the potential energy surface of G4-quadruplex – ligand complexes by computing the matrix of vibrational force constants and ensuring that it has no negative eigenvalues, i.e. frequencies, at the final optimization point [24]. We have chosen the simplest G-quadruplex model, consisting of two guanine quartet layers and a single stabilizing potassium ion [13]. As pointed out in this earlier paper of ours [13], even this simplest G-quadruplex model has 129 atoms, including  $K^+$ , to which number the atoms of the corresponding ligand have to be added. This size prevents use of higher-level explicit electron correlated methods like CCSD, and even MP2, which we use under the resolution of identity approximation, RI MP2 [13].

With the above definitions, the ligand affinity has the simple form of

$$A_{QL} = E_{QL} - (E_Q + E_L),$$

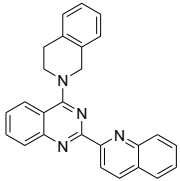
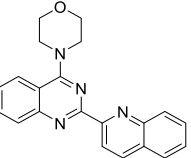
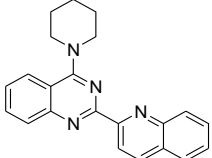
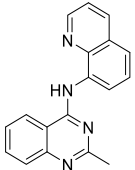
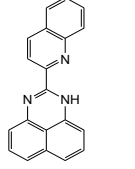
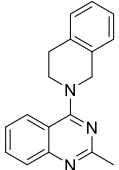
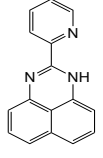
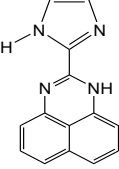
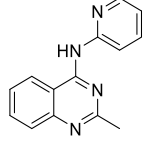
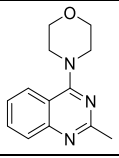
where  $E_{QL}$ ,  $E_Q$ ,  $E_L$  are the computed total energies in vacuum for the quadruplex-ligand complex, free quadruplex, and free ligand, each completely optimized at the chosen theoretical level. Computed ligand affinities have the meaning of stability constants of their G4 complexes and may be related as such to their thermodynamics. The results with the series of heterocycles [18, 19, 29] are summarized in Table 1.

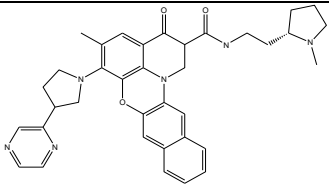
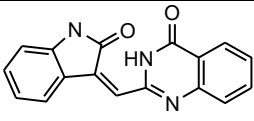
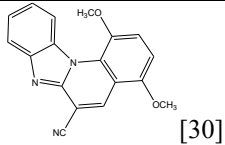
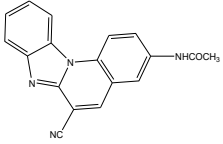
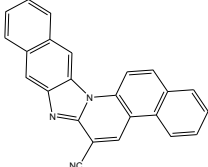
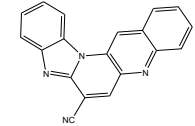
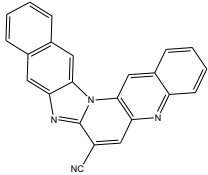
A logarithmic plot of experimental  $IC_{50}$  values [18, 19, 29] against computed DFT ligand affinities is shown in Fig. 1. Table 2 summarizes computed ligand affinities for substituted schizocommunin derivatives and their experimental biological activities [1, 28].

**Table 1.** Computed wB97XD/6-31G(d,p) total electronic energies, *hartrees*, and ligand affinities, *kcal.mol<sup>-1</sup>*, against experimentally determined  $IC_{50}$  values, *mol*, tested against the A375 line [29] entries 1-10. Some known (entries 11-14)

S. M. Bakalova, J. Kaneti: Schizocommunin analogues and derivatives as G-quadruplex ligands and anticancer agents

and hypothetical structures 15-17 illustrate trends in calculated affinities. The model quadruplex total energy E[Q2K] equals -4939.424743 hartrees. E<sub>L</sub> – ligand energy, a. u.; Q<sub>L</sub> – ligand-quadruplex energy, a. u.; A<sub>QL</sub> – affinity, kcal.mol<sup>-1</sup>.

No	Ligands	E <sub>L</sub> , a.u.	Q <sub>L</sub> , a.u.	A <sub>QL</sub> , kcal.mol <sup>-1</sup>	IC <sub>50</sub> , mol
1		-1221.484259	-6160.971209	-39.04	1.43 × 10 <sup>-5</sup>
2		-1104.982776	-6044.467535	-37.66	2.9 × 10 <sup>-5</sup>
3		-1069.087694	-6008.596043	-37.63	3.19 × 10 <sup>-5</sup>
4		-913.106098	-5852.581625	-35.20	9.8 × 10 <sup>-5</sup>
5		-933.966342	-5873.446834	-34.98	4.47 × 10 <sup>-5</sup>
6		-860.183549	-5799.660935	-33.03	5.8 × 10 <sup>-5</sup>
7		-780.369285	-5719.845155	-32.08	9.37 × 10 <sup>-5</sup>
8		-758.318366	-5697.793309	-31.53	6.05 × 10 <sup>-5</sup>
9		-759.521386	-5698.995996	-31.33	1.61 × 10 <sup>-4</sup>
10		-743.685384	-5683.152521	-26.64	1.28 × 10 <sup>-4</sup>

11	 Quarfloxin CX3543 [25]	-2007.047343	-6946.550902	-49.42	$>10^{-8}$
12	 Schizocommunin [28]	-968.888943	-5908.369172	-34.82	$>50.10^{-5}$
13	 [30]	-1008.097477	-5947.581345	-37.10	$1.10^{-6}$ HeLa [30]
14	 [31]	-987.084237	-5926.572842	-40.11	$3.10^{-6}$ HeLa [30]
15		-1086.312979	-6025.805852	-42.79	
16		-948.751257	-5888.237078	-38.33	
17		-1102.341603	-6041.834300	-42.68	

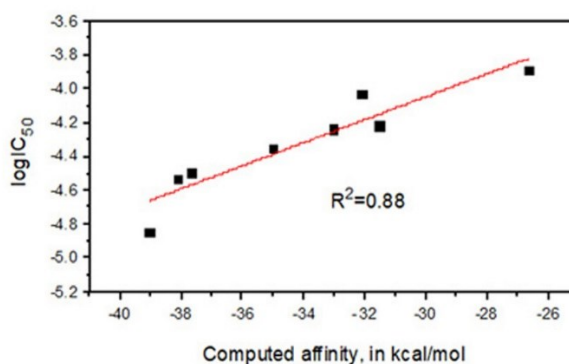
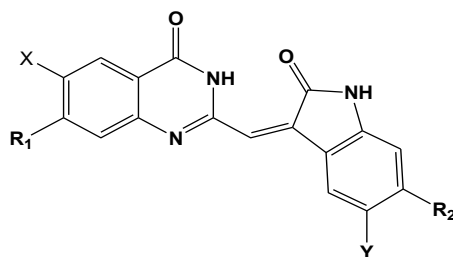


**Figure 1.** Plot of calculated wB97XD ligand affinities against the logarithm of the 50% inhibitory concentrations  $IC_{50}$  (in mol) for compounds 1–8, tested against the A375 melanoma cell line;  $R=0.9357$ ,  $R^2=0.8756$  [29].

**Table 2.** Computed M06-2x/6-31G\*\* total electronic energies in atomic units; 1 a. u. (*hartree*) = 627.51 kcal.mol<sup>-1</sup> [1] of alkaloids and schizocommunin derivatives [1, 28]. E[Q2K] = 4939.111267 *hartrees*. Affinities are in kcal.mol<sup>-1</sup>.

IC<sub>50</sub> in μmol from ref. [28]. HeLa – breast cancer cell line; U2OS – osteosarcoma cell line [28, 30]. The used compound numbering Chemn follows the original paper [28].



Substituent R <sub>n</sub>	Orig. # [28] Substit. X, Y	Ligand energy E <sub>L</sub> , a.u.	Q2K-quadruplex energy, a.u.	Affinity ΔE, kcal.mol <sup>-1</sup>	IC <sub>50</sub> HeLa, μmol	IC <sub>50</sub> U2OS, μmol
R <sub>1</sub> = -NH-(CH <sub>2</sub> ) <sub>3</sub> -NMe <sub>2</sub> R <sub>2</sub> =H	Che07 X=Y=R <sub>2</sub> =H	-1275.942614	-6215.111074	-35.51	42.5	20.4
R <sub>1</sub> =-NH-(CH <sub>2</sub> ) <sub>3</sub> -NMe <sub>2</sub> R <sub>2</sub> =H	Che08 X=F, Y=R <sub>2</sub> =H	-1375.147425	-6314.317092	-36.27	13.4	18.7
R <sub>1</sub> =-NH-(CH <sub>2</sub> ) <sub>3</sub> -N- morpholyl	Che10 X=F, Y=R <sub>2</sub> =H	-1527.727970	-6466.872389	-20.43	>50	>50
R <sub>1</sub> =-NH-(CH <sub>2</sub> ) <sub>3</sub> -NMe <sub>2</sub> R <sub>2</sub> =-N <sub>1</sub> N <sub>4</sub> Me- piperazyl	Che12 X=Y=H	-1581.866729	-6521.028646	-31.41	49	14.1
R <sub>1</sub> =-NH-(CH <sub>2</sub> ) <sub>2</sub> -NMe <sub>2</sub> R <sub>2</sub> =-N <sub>1</sub> N <sub>4</sub> Me- piperazyl	Che13 X=F, Y=H	-1681.071588	-6620.233579	-31.45	15.7	6.3
R <sub>1</sub> =-NH-(CH <sub>2</sub> ) <sub>2</sub> - tetrahydro-pyrrolyl; R <sub>2</sub> =-N <sub>1</sub> N <sub>4</sub> Me- piperazyl	Che14 X=F, Y=H	-1719.170498	-6658.332508	-31.46	17.4	6.4
R <sub>1</sub> =-N-hexahydro- pyridyl; R <sub>2</sub> =-N <sub>1</sub> N <sub>4</sub> Me- piperazyl	Che15 X=F, Y=H	-1758.462551	-6697.626406	-32.62	20.5	3.6
R <sub>1</sub> =-NH-(CH <sub>2</sub> ) <sub>3</sub> - NMe <sub>2</sub> ; R <sub>2</sub> =-N <sub>1</sub> N <sub>4</sub> Me- piperazyl	Che16 X=F, Y=H	-1681.071588	-6620.233579	-31.45	3.8	3.2
R <sub>1</sub> =-NH-(CH <sub>2</sub> ) <sub>3</sub> -NEt <sub>2</sub> ; R <sub>2</sub> =-N <sub>1</sub> N <sub>4</sub> Me- piperazyl	Che17 X=F, Y=H	-1759.662809	-6698.826612	-32.59	10.0	7.6
R <sub>1</sub> =-NH-(CH <sub>2</sub> ) <sub>3</sub> - NMe <sub>2</sub> ; R <sub>2</sub> =N-morpholyl	Che22 X=Y=F	-1760.839282	-6700.001404	-31.53	34.3	32.4
R <sub>1</sub> =-NH-(CH <sub>2</sub> ) <sub>2</sub> - tetrahydro-pyrrolyl; R <sub>2</sub> =N-morpholyl	Che23 X=Y=F	-1838.228542	-6777.394694	-34.06	>50	>50
R <sub>1</sub> =-NH-(CH <sub>2</sub> ) <sub>2</sub> -N- morpholyl; R <sub>2</sub> =N-morpholyl	Che24 X=Y=F	-1913.419817	-6852.581597	-31.32	>50	>50
R <sub>1</sub> =-N <sub>1</sub> N <sub>4</sub> Me- piperazyl; R <sub>2</sub> =N-morpholyl	Che25 X=Y=F	-1759.641803	-6698.802843	-30.86	>50	>50
R <sub>1</sub> =-NH-(CH <sub>2</sub> ) <sub>3</sub> - NMe <sub>2</sub> ; R <sub>2</sub> =-N <sub>1</sub> N <sub>4</sub> Me- piperazyl	Che30 X=Y=F	-1780.272927	-6719.435916	-32.08	17.6	9.0
R <sub>1</sub> =-NH-(CH <sub>2</sub> ) <sub>3</sub> -NEt <sub>2</sub> ; R <sub>2</sub> =-N <sub>1</sub> N <sub>4</sub> Me- piperazyl	Che31 X=Y=F	-1858.863115	-6798.028849	-33.80	9.6	6.1

R <sub>1</sub> =-NH-(CH <sub>2</sub> ) <sub>3</sub> -tetrahydro-pyrrolyl; R <sub>2</sub> =-N <sub>1</sub> N <sub>4</sub> Me-piperazyl	Che32 X=Y=F	-1857.666276	-6796.829178	-32.02	9.0	16.4
R <sub>1</sub> =-NH-(CH <sub>2</sub> ) <sub>3</sub> -N-imidazolyl; R <sub>2</sub> =-N <sub>1</sub> N <sub>4</sub> Me-piperazyl	Che33 X=Y=F	-1871.307737	-6810.469544	-31.34	>50	>50
R <sub>1</sub> =-NH-(CH <sub>2</sub> ) <sub>3</sub> N <sub>1</sub> N <sub>4</sub> -Me-piperazyl; R <sub>2</sub> =-N <sub>1</sub> N <sub>4</sub> Me-piperazyl	Che34 X=Y=F	-1952.286514	-6891.449523	-32.09	8.8	12.7
R <sub>1</sub> =-NH-(CH <sub>2</sub> ) <sub>3</sub> -NMe <sub>2</sub> ; R <sub>2</sub> =-N <sub>1</sub> N <sub>4</sub> Me-piperazyl	Che35 X=F, Y=H	-1720.357156	-6659.530943	-38.85	14.0	12.5

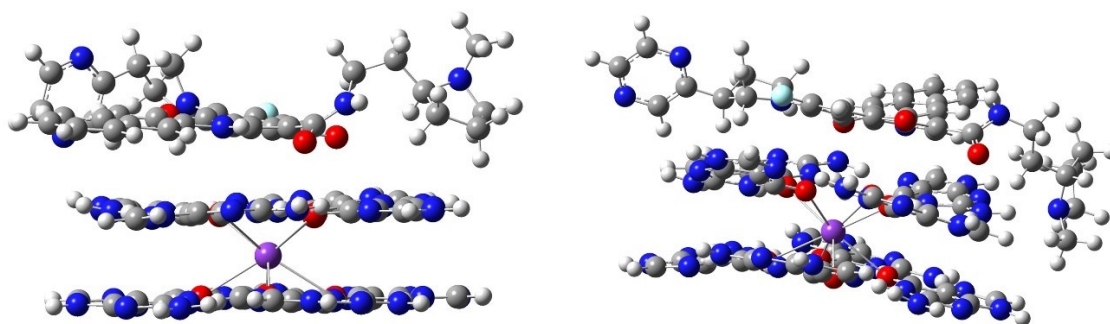


**Figure 2.** Two modes of attachment of quarfloxin [25] to a model bilayered G-quadruplex. Left: total energy -6946.550919 *hartrees*, right: total energy -6946.563341 *hartrees*. These values correspond to a difference between calculated ligand affinities of 49.5, left, and 57.3, right, *kcal.mol<sup>-1</sup>*, of *ca.* 8 *kcal.mol<sup>-1</sup>*, which is *ca.* 15% of the affinity value, defining the stacking mechanism used here. Further, more examples to this point are given by derivatives of schizocommunin, Table 2 [28].

## DISCUSSION

The clear trend revealed between experimental IC<sub>50</sub> (Inhibitory Concentration for 50% tumor suppression in present cases) of some of studied small heterocyclic ligands, Fig. 1 [29] indicates at first sight the good likeliness of the suggested stacking mechanism of their interactions with G-quadruplexes. Thus, the stacking of relatively small heterocyclic molecules to the model quadruplex “core” is probably a valid interaction mechanism, apart of known modes of NA interaction with relatively larger anticancer ligands, targeting telomeres [26, 29]. This suggestion does not eliminate by any means different modes of attachment of small heterocycles to G4 quadruplexes. The multidimensional problem of finding the minima of potential energy surfaces for these interactions has no unique solution even from the purely mathematical viewpoint. Some optimism in this direction may be found in the earlier observation that molecular dynamics G4 quadruplex potential energy surfaces are relatively flat with deep global minima for bound ligands [27]. We may then

concentrate on structural properties of small ligands and the variations of their quadruplex interaction energies elicited by ligand characteristics. A case of variations of interaction energy may arise from internal structural variations of a given ligand – the possibility of tautomeric forms and rotational isomerism. Important among the latter variations would be the changes, leading to loss of planarity of ligands, and thus to reduced affinity to G-quadruplex core stacking and deviations from the mechanism of biological interference, discussed here. An example is given on Figure 2, with two modes of attachment of CX-3543, quarfloxin [25], to a model Q2 core.

Introduction of mostly hydrophilic long-chain substituents to the leading alkaloid molecule brings additional rotatable bonds, greatly complicating the corresponding energy surface. At the same time, we attempt to find relationships between computed ligand affinities to the telomeric G-quadruplex, which is most probably responsible to observed activities of these more than thirty molecules, Table 2 [28]. These computations use the more general M06-2X/6-31G\*\* density functional. Computed M06-2X ligand affinities are similar to these of

compounds 1 – 10 (Table 1) but do not correlate with reported biological activities [28]. In fact, one has to keep in mind that our model quadruplex cannot describe the complete binding capability of this NA structure and only represents its part capable of dispersion and/or correlation interactions. There is only a part of the native quadruplex, or its model here, which is accessible by the heterocyclic ligand, which is part of the large planar surface of its internal G4 core. The surrounding part of native quadruplex can bind heterocycles too, in particular their hydrophilic substituents. This part of the affinity is comparable or possibly even larger than the part of it, which we calculate here as stacking, or dispersion, or correlation contribution to complete ligand bonding interaction, see Figure 2 for an example. Specifically, in the case of extended hydrophilic substituents, their potential interactions with pentose and phosphate residues of G4 are not covered by the present computational model. Thus, we might further be confronted with the necessity to introduce also “quadruplet accessibility” by ligands, which would give limits to their potential participation in G4 regulated bioprocesses.

## CONCLUSION

The mechanism of exerting biological activity of some aromatic heterocyclic compounds *via* formation of ligand adducts to G-quadruplexes (GQ.L) certainly finds a lot of reliable examples in biological and pharmaceutical experiments. We add to the so far formulated requirements to such heterocyclic molecules, namely crescent-like form and a number of annelated aromatic rings, preferably three or more, a quantitative measure of possible activity - the ligand affinity of heterocycles to G-quadruplexes. The latter quantitative requirement offers explanations also in cases where planarity of ligands is compromised, which reduces affinity to the G-quadruplex plane. The consequence is reduced stacking energy of the potential complex. Thus, in cases of conforming to the formulated qualitative requirements, and computed good quantitative affinity to a model G-quadruplex, we may recommend the potentially synthetically achievable molecules like entries 15 – 17 of Table 1 for further experimental studies.

**Acknowledgement:** This research was financially supported by the Bulgarian National Science Fund, Grant number KP-06-N59/1 of 15 November 2021. We gratefully acknowledge the access provided to the e-infrastructure of the NCHDC, part of the Bulgarian National Roadmap for RIs, with the financial support by Grant No D01-168 of 28.07.2022, and the Consortium Petascale

Supercomputer – Bulgaria and EuroHPC supercomputer.

## REFERENCES

1. T. Che, Y.-Q. Wang, Z.-L. Huang, J.-H. Tan, Z.-S. Huang, S.-B. Chen, *Molecules*, **23**, 493 (2018).
2. C. Chadeneau, K. Hay, H. W. Hirte, S. Gallinger, S. Bacchetti, *Cancer Res.*, **55**, 2533 (1995).
3. P. Phatak, J. C. Cookson, F. Dai, V. Smith, R. B. Gartenhaus, M. F. Stevens, A. M. Burger, *Br. J. Cancer*, **96**, 1223 (2007).
4. G. N. Parkinson, M. P. Lee, S. Neidle, *Nature*, **417**, 876 (2002).
5. M.-H. Hu, S.-B. Chen, B. Wang, T.-M. Ou, L.-Q. Gu, J.-H. Tan, Z.-S. Huang, *Nucleic Acids Res.*, **45**, 1606 (2016).
6. Y. OuYang, C. Wang, B. Zhao, H. Xiong, Z. Xiao, B. Zhang, P. Zheng, J. Hu, Y. Gao, M. Zhang, W. Zhu, S. Xu, *New J. Chem.*, **42**, 17203 (2018).
7. K.-B. Wang, M. Elsayed, G. Wu, N. Deng, M. Cushman, D. Yang, *J. Am. Chem. Soc.*, **141** (28), 11059 (2019).
8. S. Neidle, *Curr. Op. Struct. Biol.*, **19**, 239 (2009); S. Balasubramanian, L. H. Hurley, Neidle, S., *Nature Reviews Drug Discovery*, **10**, 261 (2011); S. Neidle, *J. Med. Chem.*, **59**, 5987 (2016).
9. N. Kosiol, S. Juranek, P. Brossart, A. Heine, K. Paeschke, *Molecular Cancer*, **20** (40), (2021), <https://doi.org/10.1186/s12943-021-01328-4>.
10. I. Alessandrini, M. Recagni, N. Zaffaroni, M. Folini, *Int. J. Mol. Sci.*, **22**, 5947 (2021).
11. T. Liang, X. Sun, W. Li, G. Hou, F. Gao, *Front. Pharmacol.*, **12**: 661173 (2021).
12. S. Lazareno, N. J. Birdsall, *Brit. J. Pharmacol.*, **109** (4), 1110 (1993).
13. J. Kaneti, M. Georgieva, M. Rangelov, I. Philipova, B. Vasileva, I. Angelov, D. Staneva, G. Miloshev, S. Bakalova, *BBA - General Subjects*, **1865**, 129773 (2021).
14. B. Islam, P. Stadlbauer, S. Neidle, S. Haider, J. Sponer, *J. Phys. Chem. B*, **120**, 2899 (2016).
15. J. Sponer, A. Mladek, N. Spackova, X. Cang, T. E. Grimme, S. Cheatham III, *J. Am. Chem. Soc.*, **135**, 9785 (2013).
16. P. Hohenberg, W. Kohn, *Phys. Rev.*, **136**, B864 (1964). W. Kohn, L. J. Sham, *Phys. Rev.*, **140**, A1133 (1965).
17. W. Hehre, L. Radom, P. Schleyer, J. A. Pople von R., *Ab Initio Molecular Orbital Theory*, Wiley-Interscience, 1986.
18. T. N. Moshkina, E. V. Nosova, J. V. Permyakova, G. N. Lipunova, M. S. Valova, P. Slepukhin, L. Sadieva, V. Charushin, *Dyes and Pigments*, **204**, 110592 (2022), <https://doi.org/10.1016/j.dyepig.2022.110592>
19. M. Lamperti, A. M. Giani, A. Maspero, G. Vesco, A. Cimino, R. Negri, G. B. Giovenzana, G. Palmisano, M. Mella, L. Nardo, *Journal of Fluorescence*, **29**, 495 (2019).

20. M. Hranjec, G. Pavlović, M. Marjanović, M. Kralj, G. Karminski-Zamola, *European Journal of Medicinal Chemistry*, **45**, 2405 (2010).
21. N. Perin, L. Uzelac, I. Piantanida, G. Karminski-Zamola, M. Kralj, M. Hranjec, *Bioorganic & Medicinal Chemistry*, **19**, :6329 (2011).
22. S. Grimme, *J. Chem. Phys.*, **118**, 9095 (2003).
23. J.-D. Chai, M. Head-Gordon, *Phys. Chem. Chem. Phys.*, **10**, 6615 (2008).
24. Gaussian 16, Revision C.01, M. J. Frisch, G. W. Trucks; H. B. Schlegel, G. E. Scuseria, M. A. Robb, J. R. Cheeseman, G. Scalmani, V. Barone, G. A. Petersson, H. Nakatsuji, X. Li, M. Caricato, A. V. Marenich, J. Bloino, B. G. Janesko, R. Gomperts, B. Mennucci, H. P. Hratchian, J. V. Ortiz, A. F. Izmaylov, J. L. Sonnenberg, D. Williams-Young, F. Lipparini, F. Egidi, J. Goings, B. Peng, A. Petrone, T. Henderson, D. Ranasinghe, V. G. Zakrzewski, J. Gao Ding, N. Rega, G. Zheng, W. Liang, M. Hada, M. Ehara, K. Toyota, R. Fukuda, J. Hasegawa, M. Ishida, T. Nakajima, Y. Honda, O. Kitao, H. Nakai, T. Vreven, K. Throssell, J. A. Montgomery Jr., J. E. Peralta, F. Ogliaro, M. J. Bearpark, J. J. Heyd, E. N. Brothers, K. N. Kudin, V. N. Staroverov, T. A. Keith, R. Kobayashi, J. Normand, K. Raghavachari, A. P. Rendell, J. C. Burant, S. S. Iyengar, J. Tomasi, M. Cossi, J. M. Millam, M. Klene, C. Adamo, R. Cammi, J. W. Ochterski, R. L. Martin, K. Morokuma, O. Farkas, J. B. Foresman, D. J. Fox, Gaussian, Inc., Wallingford CT, 2019.
25. D. Drygin, A. Siddiqui-Jain, S. O'Brien, M. Schwaebe, A. Lin, J. Bliesath, C. B. Ho, C. Proffitt, K. Trent, J. P. Whitten, J. K. C. Lim, D. Von Hoff, K. Anderes, W. G. Rice, *Cancer Res.*, **69**(19), 7653 (2009).
26. S. Asamitsu, S. Obata, Z. Yu, T. Bando, H. Sugiyama, *Molecules*, **24**, 429 (2019).
27. B. Machireddy, H.-J. Sullivan, C. Wu, *Molecules*, **24**, 1010 (2019).
28. T. Che, S.-B. Chen, J.-L. Tu, B. Wang, Y.-Q. Wang, Y. Zhang, J. Wang, Z.-Q. Wang, Z.-P. Zhang, T.-M. Ou, Y. Zhao, J.-H. Tan, Z.-S. Huang, *J. Med. Chem.*, **61**, 3436 (2018).
29. J. Kaneti, V. Kurteva, M. Georgieva, N. Krasteva, G. Miloshev, N. Tabakova, Z. Petkova, S. Bakalova, *Molecules*, **27**, 7577 (2022).
30. M. Hranjec, G. Pavlovic, M. Marjanovic, M. Kralj, G. Karminski-Zamola, *Eur. J. Med. Chem.*, **45**, 2405 (2010).
31. N. Perin, L. Uzelac, I. Piantanida, G. Karminski-Zamola, M. Kralj, M. Hranjec, *Bioorg. Med. Chem.*, **19**, 6329 (2011),